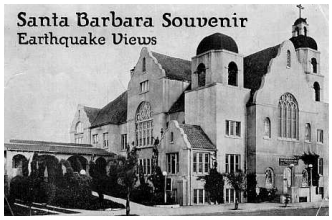

4th IASPEI / IAEE International Symposium:

Effects of Surface Geology on Seismic Motion

August 23–26, 2011 · University of California Santa Barbara

DIFFUSE FIELDS IN LAYERED MEDIA

Francisco J. SÁNCHEZ-SESMA
Instituto de Ingeniería, Universidad Nacional Autónoma de Mexico
Coyoacan, DF 04510
MEXICO

Hiroshi KAWASE
Disaster Prev. Research Institute
University of Kyoto
Gokasho, Uji
JAPAN

Shinichi MATSUSHIMA
Disaster Prev. Research Institute
University of Kyoto
Gokasho, Uji
JAPAN

ABSTRACT

For an elastic medium under diffuse seismic illumination the average cross correlation of motions at pairs of receivers, in frequency domain, is proportional to the imaginary part of Green function. At the loading zone this quantity is proportional to the power injected into the medium by a unit load and varies due to waves reflected back to the source location. Here we consider layered media and two extreme cases; the 3D for microtremors and the 1D for deep sources. The motions associated to coda waves and to seismic noise reveal multiple scattering. Its intensities are governed by diffusion-like equations. Microtremors are generated near the surface and we assume they constitute a diffuse seismic field. Thus, we link energy densities with 3D Green function. This allows the inversion of shallow structure from the microtremor *H/V* spectral ratio, the well known Nakamura's ratio. When deep earthquakes illuminate the site from below body waves predominate. We assume that autocorrelations, averaged for several earthquakes, represent energy densities which are proportional to the imaginary part of 1D Green function at the free surface, which is proportional to the squared amplitude of the corresponding transfer function for a vertically incident plane wave. This also allows for structure inversion from average earthquake *H/V* spectral ratios.

INTRODUCTION

The effects of surface geology can produce significant changes in earthquake ground motion and induce damage (Sánchez-Sesma 1987; Aki 1988). Spectral ratios of recorded motions relative to a reference rock site are useful to characterize such effects (*e.g.* Cadet *et al.* 2010). These empirical transfer functions (ETF) and can be easily obtained for seismically active locations. In most cases the ETF are interpreted using a 1D soil structure. Giving a 1D soil structure a theoretical transfer function can be obtained.

Lermo and Chávez-García (1994) obtained reliable estimates of the soil frequency from the spectral ratio between horizontal and vertical motions of microtremors. Usually the Noise H/V spectral ratio (NHV) reveals the site dominant frequency f_0 but the amplitude is not well understood (Pilz *et al.* 2009). An important step towards the understanding of the NHV is the recent work of Lunedei and Albarello (2010). They computed NHV considering a distribution of random surface sources in a weakly dissipative layered medium.

The ratio H/V became very popular but also has remained as a puzzle. For instance, it was assumed that microtremors were mainly composed of surface waves. In fact, the ratio H/V has been related to Rayleigh waves ellipticity (Lermo and Chávez-García 1994; Malischewsky and Scherbaum 2004). When Rayleigh and Love waves come from various directions the ellipticity has no clear physical meaning. However, successful inversion schemes are based on surface waves ellipticity (Arai and Tokimatsu 2004; Cadet 2007). Others propose more body waves around the peak of the H/V (Nakamura 2000; Bonnefoy-Claudet *et al.* 2008; Herat 2008).

In a recent study it was assumed that the noise is a diffuse wavefield containing all types of elastic waves (Sánchez-Sesma *et al.* 2010; 2011a). This allows relating field measurements and the Green's function (GF) which is an intrinsic property of the system (see e.g. Campillo and Paul 2003; Weaver and Lobkis 2004; Sánchez-Sesma and Campillo 2006; Sánchez-Sesma *et al.* 2008). In fact, it implies the proportionality between the average energy densities of a diffuse field and the imaginary part of GF at the source (Sánchez-Sesma *et al.* 2008; Perton *et al.* 2009). Thus, the NHV can be computed in terms of certain imaginary parts of Green tensor components. This theory explains experimental and theoretical results. According to the principle of equipartition it is possible to establish that within a

diffuse field all modes carry the same energy (Margerin 2009; Tsai 2010). The assumption of the diffuse character of microtremors requires further scrutiny. In the meantime, it seems that this hypothesis is not in conflict with the 3D nature of Green's function. It is clear that microtremors are a surface-related phenomenon. In fact, Albarello and Lunedei (2011) obtained NHV explicitly from the total elastic field radiated by a random distribution of surface point-like harmonic sources.

On the other hand, we conducted a parallel research considered strong ground motion in elastic layered media (Kawase *et al.* 2011) and explored the theoretical consequences of assuming both a flat layered site and various earthquake sources that are "sufficiently" deep, so that surface waves are not dominant or do not appear yet in the target windows. Certainly, surface waves may carry most of the effects of lateral heterogeneity and they have certainly a three dimensional (3D) nature. Excluding these waves we strictly enforce the one dimensional (1D) wave propagation. In any event, the average spectral densities of seismic motions are assumed to be depth dependent. Thus, autocorrelations can be related through the diffuse field formalism to the imaginary part of the 1D Green's function for source and receiver at the same point. The illumination at depth in the average has its spectral response around the null wave number. This problem was precisely the one tackled by Clearbout (1968). For 1D layered media he discovered the relationship between reflection response and autocorrelation of surface motion. Based on this Scherbaum (1987) developed an algorithm to identify reflection coefficients. He used records of small earthquakes in Germany to identify the subsurface site structure. These pioneering results have been interpreted under the light of diffuse field concepts and considerable simplifications have been proposed (Kawase *et al.* 2011). For instance, an extension of Claerbout's (1968) result is the finding that the imaginary part of the 1D Green function at the surface for a surface source is proportional to the square of the transfer function for an incoming unit wave.

This result also holds for the illumination due to earthquakes. In fact, it can be applied for *average* horizontal-to-vertical (*H/V*) spectral ratio of earthquake motions. To verify this relationship, Kawase *et al.* (2011) modeled such a diffuse wave field and considered a set of incoming plane waves (of P, SV, and SH types) with varying azimuths, incidence, and polarization angles covering the half-space underlying a layered medium.

In what follows some remarks are made for multiple scattering and diffuse fields. Very briefly the connection is established between average autocorrelations and the Green's function in 3D. The result for 1D excitation is given as well. These two extreme cases of spectral ratio *H/V* show (a) the use of microtremors with a 3D description for inversion of shallow structure and (b) how deep sources may allow structure inversion using 1D modeling. These descriptions emerge from the theory of diffuse fields.

DIFFUSE FIELDS IN DYNAMIC ELASTICITY

If within an inhomogeneous, elastic, anisotropic medium a set of uncorrelated random forces is acting then the correlation properties of the resulting field and those of a multiply-scattered wave field are entirely equivalent. Since the later are well described by diffusion-like equations, we employ the term *diffuse* for the noise wave field. A remarkable result is that under these circumstances the GF can be retrieved from averaging cross correlations of the recorded motions (Campillo and Paul 2003; Sánchez-Sesma *et al.* 2008).

The relationships among energy densities and autocorrelations have been recently studied by Perton *et al.* (2009) and by Margerin *et al.* (2009). The *average autocorrelation* of a diffuse field for given direction and position is proportional to the *directional energy density* (DED). Directional energy densities have been explored further and the connection between deterministic results (regarding energy partitions in a half-space due to surface loads) and diffuse fields has been clearly established (Sánchez-Sesma *et al.* 2011b).

THE RETRIEVAL OF THE GREEN'S FUNCTIONS FROM CORRELATIONS

It is now well known (see e. g. Perton *et al.* 2009) that if a 3D diffuse, equipartitioned, harmonic displacement vector field $u_i(\mathbf{x},\omega)$ is established within an elastic medium, then the average cross-correlations of motions at points $\mathbf{x_A}$ and $\mathbf{x_B}$ can be written as:

$$\left\langle u_i(\mathbf{x_A},\omega)u_j^*(\mathbf{x_B},\omega)\right\rangle = -2\pi E_S k^{-3}\,\mathrm{Im}\left[G_{ij}(\mathbf{x_A},\mathbf{x_B},\omega)\right] \tag{1}$$

where the Green's Function $G_{ij}(\mathbf{x_A},\mathbf{x_B},\omega)$ = displacement at $\mathbf{x_A}$ in direction *i* produced by a unit harmonic load acting in direction *j* at point $\mathbf{x_B}$ expressed by $\delta_{ij}\delta(|\mathbf{x}-\mathbf{x_B}|)\exp(\mathrm{i}\omega t)$, $\mathrm{i}=\sqrt{-1}$ = imaginary unit, ω = circular frequency, t = time, $k=\omega/\beta$ = shear wave number, β = shear wave propagation velocity, $E_S=\rho\omega^2S^2$ = average energy density of shear waves which is a measure of the strength of the diffuse illumination, ρ = mass density, and S^2 = average spectral density of shear waves. The angular brackets denote

azimuthal average and the asterisk* means complex conjugate.

ENERGY DENSITIES AT GIVEN POINTS AND DIRECTIONS

Assuming $\mathbf{x_A} = \mathbf{x_B}$ in Eq. 1 the total energy density at point $\mathbf{x_A}$ can be obtained by means of:

$$E(\mathbf{x_A}) = \rho\omega^2 \left\langle u_m(\mathbf{x_A}) u_m^*(\mathbf{x_A}) \right\rangle = -2\pi\mu E_S k^{-1} \times \mathrm{Im}[G_{mm}(\mathbf{x_A}, \mathbf{x_A})] \tag{2}$$

This energy density is proportional to the imaginary part of the trace of the Green tensor for coincident receiver and source. The imaginary part represents the power injected by the unit harmonic load. This quantity reveals energies that are both radiated and coming back to the source and may be used for imaging. Eq. 2 is valid even if the summation convention is ignored (Perton *et al.* 2009). In that case $E(\mathbf{x_A}) \equiv E_m(\mathbf{x_A})$ = *directional energy density* (DED) along direction *m*.

THE *H/V* SPECTRAL RATIO FOR MICROTREMORS

Assume that microtremors constitute a diffuse field. Then, the average spectral densities may be regarded as *directional energy densities* (DEDs). It is common to eliminate the angular brackets while writing the expression for the average *H/V* spectral ratio as:

$$\frac{H(\omega)}{V(\omega)} = \sqrt{\frac{E_1(\mathbf{x},\omega) + E_2(\mathbf{x},\omega)}{E_3(\mathbf{x},\omega)}}, \tag{3}$$

where E_1, E_2 and E_3 are the DEDs and the subscripts 1 and 2 refer to horizontal and the 3 to vertical degrees of freedom (*e.g.* Arai and Tokimatsu 2004). Following Sánchez-Sesma *et al.* (2011a) we express the NHV from Eqs. 2 and 3. Thus we can write

$$\frac{H(\omega)}{V(\omega)} = \sqrt{\frac{\mathrm{Im}[G_{11}(\mathbf{x},\mathbf{x};\omega)] + \mathrm{Im}[G_{22}(\mathbf{x},\mathbf{x};\omega)]}{\mathrm{Im}[G_{33}(\mathbf{x},\mathbf{x};\omega)]}}. \tag{4}$$

This equation (Sánchez-Sesma *et al.* 2011a) relates *average* measurements with an *intrinsic* property of the medium and allows for the inversion of *H/V*, the Nakamura's ratio. Appendix A describes how to compute the imaginary part of Green functions at the source.

THE *H/V* SPECTRAL RATIO FOR EARTHQUAKES

For most earthquakes, the local structure around the observation site will be illuminated mainly by plane body waves from the source with multiple reflections and refractions, as shown schematically in Figure 1. This implies that ground motions are composed essentially of plane waves (Kawase *et al.* 2011). Moreover, if the medium has only depth-dependent properties we assume statistical equivalence of horizontal directions. Consequently, we describe the problem as 1D. Thus, from Eq. 2 and assuming **x**=0 we can write:

$$\left\langle H^2 \right\rangle \propto \mathrm{Im}[G_{11}^{1D}(0,0;\omega)] + \mathrm{Im}[G_{22}^{1D}(0,0;\omega)], \quad \text{and } \left\langle V^2 \right\rangle \propto \mathrm{Im}[G_{33}^{1D}(0,0;\omega)] \tag{5}$$

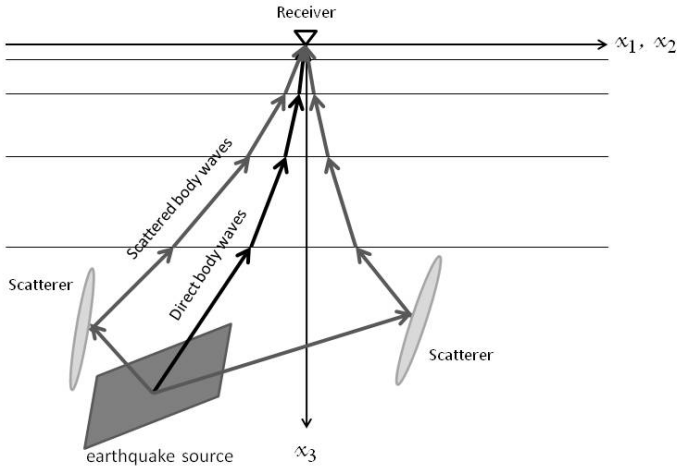

Fig. 1. Schematic illustration of direct and scattered wave field illuminated by

deep earthquake sources in a 1D layered half space (after Kawase et al. 2011).

where $E_1 + E_2 = \langle H^2 \rangle$, and $\mathrm{E}_3 = \langle V^2 \rangle$ are the averages of the horizontal and vertical autocorrelations, respectively, and $G_{ij}^{1D}(\mathbf{x},\mathbf{y};\omega)$ = the Green function of the 1D structure at the circular frequency ω. For the coordinate suffix i and j, we use 1 and 2 for the two horizontal directions, while 3 for the vertical direction. As before, we write the average *H/V* spectral ratio as follows:

$$\frac{H(\omega)}{V(\omega)} = \sqrt{\frac{\mathrm{Im}[G_{11}^{1D}(0,0;\omega)] + \mathrm{Im}[G_{22}^{1D}(0,0;\omega)]}{\mathrm{Im}[G_{33}^{1D}(0,0;\omega)]}} \tag{6}$$

Equations 4 and 6 are fundamental; they are direct consequences of the diffuse wave theory for Green's function retrieval, when the two observation points coincide (i.e., autocorrelation is taken). Consider Eq. 6 and from Appendix B specialize Eq. B6. We find the transfer function for horizontal motion due to S wave, $TF_1(\omega)$, while for the P motion we have $TF_3(\omega)$. We may write

$$\frac{H(0,\omega)}{V(0,\omega)} = \sqrt{\frac{2\alpha_H}{\beta_H}} \frac{|TF_1(0,\omega)|}{|TF_3(0,\omega)|}, \tag{7}$$

where we added zero inside the parenthesis to represent the depth of the source and receiver at the surface.

RESULTS FROM THE TWO DESCRIPTIONS

In order to clarify from the theoretical point of view how these descriptions work we study two models that are relatively simple: Model A is single layer over a half space while model B has three distinct layers over the half-space. The layer's thicknesses and the compressional and shear wave velocities are given in Table 1. Note that α, the P wave speed, was left unchanged in both models. In model B the assumed three layers have different values of β, the S wave speed. Density is assumed unit in both models.

Table 1. Description of models

Model A			Model B		
Thickness (m)	α (m/s)	β (m/s)	Thickness (m)	α (m/s)	β (m/s)
10	500	100	5	500	30
10	500	100	25	500	100
10	500	100	50	500	150
∞	1500	500	∞	1500	500

In Fig. 2 the imaginary parts of Green functions $G_{11}(0,0;\omega)$ and $G_{33}(0,0;\omega)$ at the surface are depicted *versus* frequency. The left panel shows the growing tendency with increasing frequency. Both responses display a smooth increase from zero that suggests no radiation at low frequency. For increased frequency an overshoot appears in vertical response and then a linear grow is appreciated. The

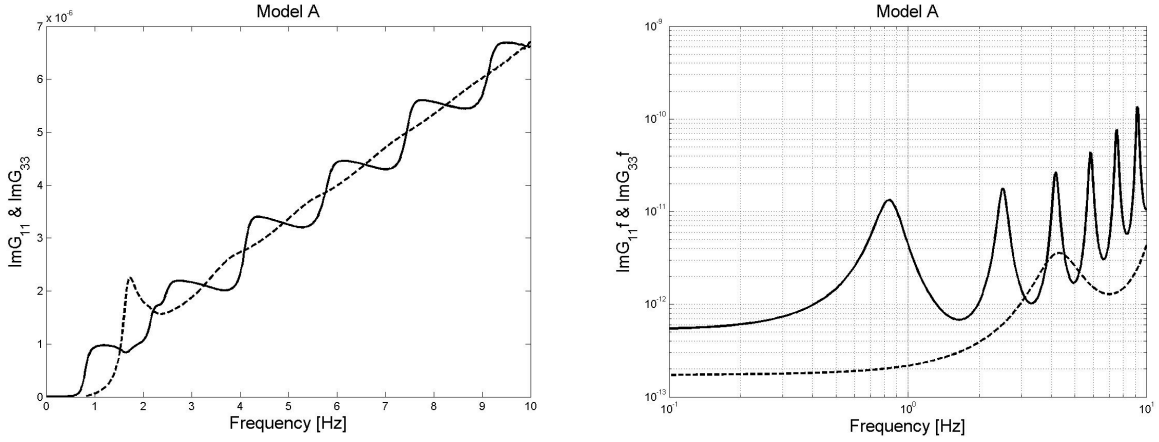

Figure 2. Imaginary part of Green functions at the surface. 3D and 1D cases in the left and right panels. Continuous and dotted lines correspond to horizontal and vertical responses. The right panel shows the imaginary part of Green's functions at the surface times the frequency.

horizontal response shows jumps that appear at the layer's resonant frequencies in Hz (0.833, 2.5, 4.166, …). This quantum-like behavior in the horizontal response can be explained by the fact that most than 2/3 of the energy injected into the medium by a horizontal load is carried by body shear waves, thus the consequent resonances clearly show up. The vertical response first overshoot has no clear meaning. It appears at a frequency of about twice the *H/V* peak. It seems to be independent of the P wave speed in the layer. However, as frequency grows $\mathrm{Im}G_{33}$ behaves as linear function of frequency in the same way as the solution for a half-space with the properties of the uppermost layer. This also can be explained by the significant radiation of Rayleigh waves by a normal load and with growing frequency these waves reduce their penetration with depth. These are deterministic results for energy partitions in a half-space due to surface loads (Sánchez-Sesma *et al.* 2011b). The case of 1D response is depicted in the right panel of Fig. 2. It shows $\mathrm{Im}\,G_{11}^{1D} f$ and $\mathrm{Im}\,G_{33}^{1D} f$ and therefore we can recognize the square of 1D transfer functions. In both cases one can clearly distinguish the higher modes of Love waves.

From Eq. 4 we can obtain the ratio *H/V* that is depicted in the left panel of Fig. 3. A peak is clearly seen at the resonant frequency $f_0=\beta/4h$=0.8333Hz. Note that the peak comes from the ratio of two functions that are growing. The manifestations of higher modes are

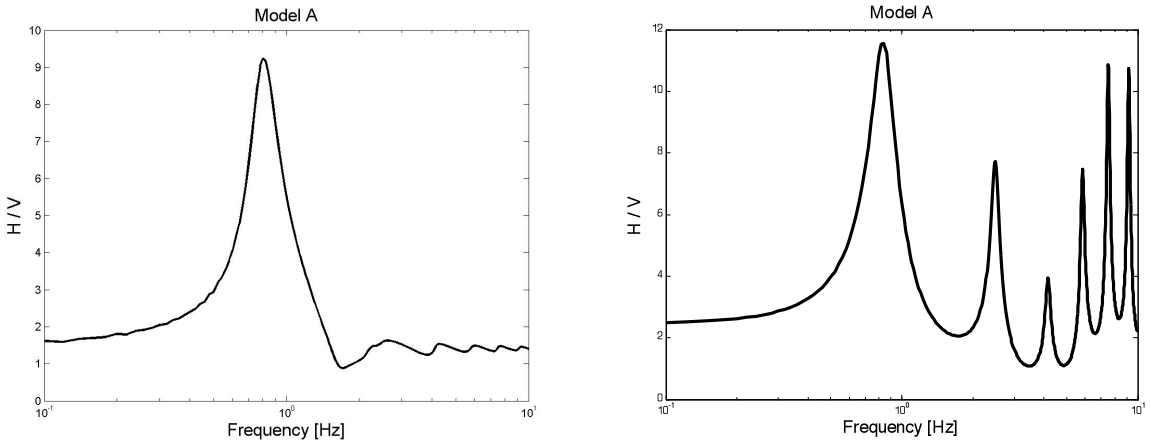

Fig. 3. H/V for both microtremors (left) and deep sources (rigth). Results for Model A

flattened by the quotient (see the left panel of Fig. 2). On the other hand the right panel of Fig. 3 depicts *H/V* computed for Model A from Eq. 7. The asymptotic value for low frequencies $\sqrt{2\alpha_H/\beta_H}=\sqrt{2\times1500/500}=2.45$ and the peaks oh higher modes are preserved. Note that the small amplitude of third peak is due to the coincidence of first peak of P response.

Model B has three layers with different thicknesses and speeds of shear waves in each layer. The 3D and 1D descriptions of Appendixes A and B allowed us to compute the imaginary parts of Green's functions at the free surface. The results are depicted in the left and right panels of Fig. 4. The continuous line corresponds to the horizontal response while dotted lines depict the vertical one. The use of frequency as a factor enhances the characteristics of 1D responses.

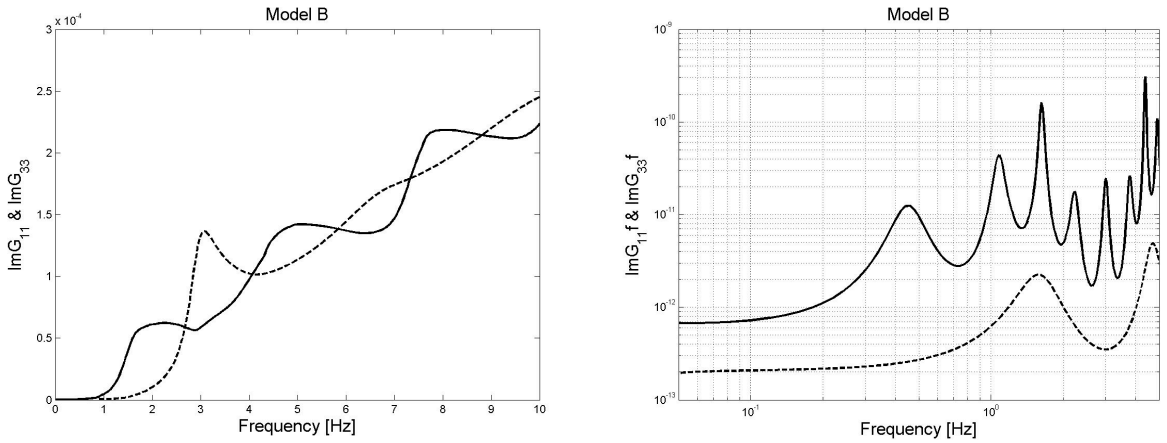

Fig. 4. Imaginary parts of Green functions at the surface of Model B. The results for microtremors are in the left panel. For deep sources (right panel) the plots are the ImG values multiplied by frequency. Continuous

line corresponds to the horizontal response and dotted depict the vertical one.

The corresponding *H/V* spectra are displayed in Fig. 5. In the left panel, the results correspond to microtremors (3D description). Two conspicuous peaks appear at frequencies 0.45 and 1.50 Hz. These peaks come from the ratios of $\mathrm{Im}G_{11}$ and $\mathrm{Im}G_{33}$ which are each growing functions with frequency around that values. The first one corresponds precisely to the fundamental mode but a second peak at 1.5 Hz should be associated to the "local" response of the uppermost layer. For larger frequencies the response is flattened.

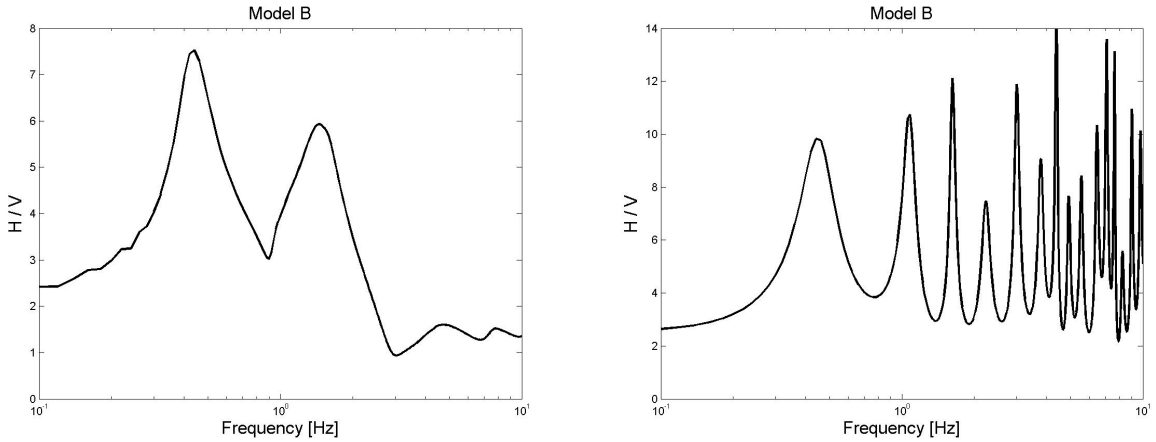

Fig. 5. H/V for both microtremors (left) and deep sources (rigth). Results for Model B.

The right panel of Fig. 5 depicts *H/V* computed for Model B from Eq. 7 (1D description). The asymptotic value for low frequencies is the same as in model A because the half-space is the same. Many peaks show up that reveal increased complexity in this three layer system as compared with the single layer model. Only the first peak at a frequency of 0.45Hz coincides in both descriptions.

DISCUSSION AND CONCLUSIONS

These results for *H/V* spectra show the distinct character of two extreme descriptions of diffuse waves in simple layered systems. The one associated to microtremors is closer to the 3D behavior and this appears to be more sensitive to shallow structure. For the response due to deep sources several modes are excited; the illumination from bellow gives, when the averages of autocorrelations are obtained, an interesting relationship with 1D responses to P and S waves, respectively.

The stabilization of the normalized average autocorrelation for a given energy level suggests that the resulting illumination is equipartitioned (Sánchez-Sesma, *et al.* 2011a). We assume that the resulting spectra can be regarded as specific 3D or 1D signatures of the site. The *H/V* spectra can be expressed in terms of a quotient that includes the imaginary part of GF components at the source.

Our formulation in 3D naturally allows for the inversion of the Nakamura's (1989) ratio. The GF includes all the contributions of Rayleigh, Love and body waves. We are currently investigating if partial equipartition and attenuation imply limits to our approach. We expect that with this scheme the residuals in inversion become smaller than those for other approaches.

We interpret diffuse field theory liberally and assume that various deep events of similar energy levels may be parts of a diffuse field.

By averaging the horizontal and vertical motions for microtremors and deep sources, the inversion of a layered structure is possible. The average of deep earthquakes may provide good illumination, useful to inversion.

ACKNOWLEDGEMENTS

Thanks are given to D.Albarello, P.-Y. Bard, K. Irikura, U. Iturrarán-Viveros, E. Lunedei, L. Margerin, H. Sato and T. Yokoi for enlightening discussions. G. Sánchez N. and her team from USI-II-UNAM, found useful references. G. Aguirre helped in various stages of this work. Supports from DGAPA-UNAM, Project IN121709, Mexico is greatly appreciated.

REFERENCES

Aki, K. and P.G. Richards [1980], "Quantitative Seismology. Theory and Methods", W. H. Freeman, San Francisco.

Aki, K. [1988], "Local Site Effects on Strong Ground Motion", in "*Earthquake Engineering and Soil Dynamics I --Recent Advance in Ground*

Motion Evaluation", J. L. Von Thun (Ed.), Geotech. Special Pub. No. 20, ASCE, New York, pp. 103-155.
Albarello, D., E. Lunedei [2011]. "Structure of an ambient vibration wavefield in the frequency range of emgineering interest ([0-5, 20]Hz): insights from numerical modelling", Near Surface Geophys. Vol. 9, pp – , In press.

Arai, H., and K. Tokimatsu [2004], "S-Wave Velocity Profiling by Inversion of Microtremor H/V Spectrum", Bull. Seism. Soc. Am., Vol. 94, No. 1, pp. 53–63.

Bard, P-Y [2008] "The H/V Technique: Capabilities and Limitations Based on the Results of the SESAME Project", Bull. Earthq. Eng. Vol 6, pp. 1–2.

Bonnefoy-Claudet, S., C. Cornou, P.-Y. Bard, F. Cotton, P. Moczo, J. Kristek, and D. Fäh [2006], "H/V Ratio: a Tool for Site Effects Evaluation. Results From 1-D Noise Simulations", Geophys. J. Int., Vol. 167, pp. 827-837.

Bonnefoy-Claudet S., A. Köhler, C. Cornou, M. Wathelet, and P.-Y Bard [2008]. "Effects of Love Waves on Microtremor H/V Ratio", Bull. Seism. Soc. Am., Vol. 98, No. 1, pp. 288–300.

Cadet, H. [2007], "*Utilisation Combinée des Méthodes Basées sur le Bruit de Fond Dans le Cadre du Microzonage Sismique*", PhD Thesis, Univ. J. Fourier, Grenoble, France.

Cadet, H., P-.Y. Bard, and A. Rodriguez-Marek [2010], "Defining a Standard Rock Site: Propositions Based on the KiK-net Database", Bull. Seism. Soc. Am. Vol. 100, No. 1, pp. 172-195.

Campillo, M. and A. Paul 2003. "Long range correlations in the seismic coda", Science **299**, 547-549.

Fäh, D., F., Kind, and D., Giardini [2001]. "A theoretical Investigation of Average H/V Ratios", Geophys. J. Int. Vol. 145, pp. 535–549.

Herat, M. [2008]. "Model HVSR - A Matlab® Tool to Model Horizontal-to-Vertical Spectral Ratio of Ambient Noise", Computers & Geosciences. Vol. 34, pp. 1514–1526.

Kawase, H., F. J. Sánchez-Sesma and S. Matsushima [2011]. "The optimal use of Horizontal-to-Vertical spectral ratios of earthquake motions for velocity structure inversions based on diffuse field theory for plane waves", Bull. Seism. Soc. Am., Vol. 101, pp - . In press.

Kennett, B.L.N., [2001]. "The Seismic Wavefield. Volume 1: Introduction and Theoretical Development", Cambridge University Press. Cambridge.

Knopoff, L [1964]. "A Matrix Method for Elastic Wave Problems", Bull. Seism. Soc. Am., Vol. 54, pp. 431-438.

Konno, K. and T., Ohmachi [1998]. "Ground-Motion Characteristics Estimated from Spectral Ratio between Horizontal and Vertical Components of Microtremor", Bull. Seism. Soc. Am., Vol. 88, pp. 228-241.

Lermo, J. and F.J., Chávez-García [1994]. "Are Microtremors Useful in Site Response Evaluation?", Bull. Seism. Soc. Am., Vol. 84, pp. 1350-1364.

Lunedei, E. and D., Albarello [2010]. "Theoretical HVSR Curves from Full Wavefield Modelling of Ambient Vibrations in a Weakly Dissipative Layered Earth", Geophys. J. Int. Vol. 181, pp. 1093–1108,

Malischewsky, P.G. and F., Scherbaum [2004]. "Love's Formula and H/V-Ratio (Ellipticity) of Rayleigh Waves", Wave Motion, Vol. 40, pp. 57-67.

Margerin, L. [2009]. "Generalized Eigenfunctions of Layered Elastic Media and Application to Diffuse Fields", J. Acoust. Soc. Am., Vol. 125, pp. 164-174.

Margerin, L., Campillo, M., B.A., van Tiggelen, and R., Hennino [2009]. "Energy Partition of Seismic Coda Waves in Layered Media: Theory and Application to Pinyon Flats Observatory, Geophys. J. Int., Vol 177, pp 571-585.

Nakamura, Y [1989]. "A Method for Dynamic Characteristics Estimation of Subsurface Using Microtremor on the Ground Surface", Quaterly Rep. Railway Tech. Res. Inst., Vol. 30, pp. 25-30.

Nakamura, Y [2000]. "Clear identification of fundamental idea of Nakamura's technique and its applications". Proc. 12th World Conf. on Earthq. Eng., New Zeland (CD-ROM), pp. 8.

Perton, M., F.J., Sánchez-Sesma, A., Rodríguez-Castellanos, M., Campillo and R.L., Weaver [2009]. "Two Perspectives on Equipartition in Diffuse Elastic Fields in Three Dimensions", J. Acoust. Soc. Am., Vol. 126, pp. 1125-1130.

Pilz, M., S., Parolai, F., Leyton, J., Campos, and J., Zschau [2009]. Techniques Using Earthquake Data and Ambient Seismic Noise Analysis in the Large Urban Areas of Santiago de Chile", Geophys. J. Int., Vol. 178, Num. 2, pp. 713-728.

Sánchez-Sesma, F.J [1987]. "Site Effects on Strong Ground Motion", Soil Dyn. Earthq. Eng., Vol. 6, pp. 124- 132.

Sánchez-Sesma, F.J. and M., Campillo [2006]. "Retrieval of the Green Function from Cross-Correlation: The Canonical Elastic Problem", Bull. Seism. Soc. Am., Vol. 96, pp. 1182-1191.

Sánchez-Sesma, F. J., J. A., Pérez-Ruiz, M., Campillo, and F., Luzón [2006]. "The Elastodynamic 2D Green Function Retrieval from Cross-Correlation: Canonical Inclusion Problem", Geophys. *Res. Lett.,* Vol. 33*,* No. 13305, pp. 1 – 6.

Sánchez-Sesma, F.J., J.A., Pérez-Ruiz, F., Luzón, M., Campillo and A., Rodríguez-Castellanos [2008]. "Diffuse Fields in Dynamic Elasticity", Wave Motion, Vol. 45, pp. 641–654.

Sánchez-Sesma, F. J., M., Rodríguez, U., Iturrarán-Viveros, A., Rodríguez-Castellanos, M., Suarez, M. A., Santoyo, A., García-Jerez, and F., Luzón [2010]. "Site Effects Assessment Using Seismic Noise", in "Proc. 9th International Workshop on Seismic Microzoning and Risk Reduction", 21st - 24th February, Cuernavaca, Mexico.

Sánchez-Sesma, F.J., M., Rodríguez, U., Iturrarán-Viveros, F., Luzón, M. ,Campillo, L., Margerin, A., García-Jerez, M., Suárez, M. A., Santoyo, and A., Rodríguez-Castellanos [2011a]. "A Theory for microtremor H/V Spectral ratio: Application for a layered médium", Geophysical Journal International, Vol. 186, pp 221-225.

Sánchez-Sesma, F. J., R. L., Weaver, H., Kawase, S., Matsushima, F., Luzón, and M., Campillo [2011b]. "Energy Partitions Among Elastic Waves for Dynamic Surface Loads in a Semi-Infinite Solid", Bull. Seism. Soc. Am., Vol. 101, In press, doi:10.1785/0120100196.

Sato, H. [2010]. "Retrieval of Green's Function Having Coda Waves from the Cross-Correlation Function in a Scattering Medium Illuminated by a Randomly Homogeneous Distribution of Noise Sources on the Basis of the First-Order Born Approximation" Geophys. J. Int. Vol. 180, pp. 759–764.

Weaver, R.L. [1982]. "On Diffuse Waves in Solid Media", J. Acoust. Soc. Am., Vol. 71, pp. 1608-1609.

Weaver, R.L. [1985]. "Diffuse Elastic Waves at a Free Surface", J. Acoust. Soc. Am., Vol. 78, pp. 131–136.

Weaver, R.L. and O.I., Lobkis [2004]. "Diffuse Fields in Open Systems and the Emergence of the Green's Function", J. Acoust. Soc. Am., Vol. 116, pp. 2731-2734.

Yokoi, T. and S., Margaryan [2008]. "Consistency of the Spatial Autocorrelation Method with Seismic Interferometry and its Consequence", Geophys. Prospecting*,* Vol. 56, pp. 435–451

APPENDIX A

THE IMAGINARY PART OF GREEN FUNCTION AT THE SURFACE LOAD POINT. THE LAYERED 3D ELASTIC CASE

Consider a 3D layered medium. Assume a set of *N* horizontal elastic layers overlaying a half-space. Layer *j* is defined at $z_j \le z \le z_{j+1}$ such that $h_j = z_{j+1} - z_j$ = thickness of layer. The top layer has $z_1 = 0$, while z_{N+1} is the half-space top (see Fig. A).

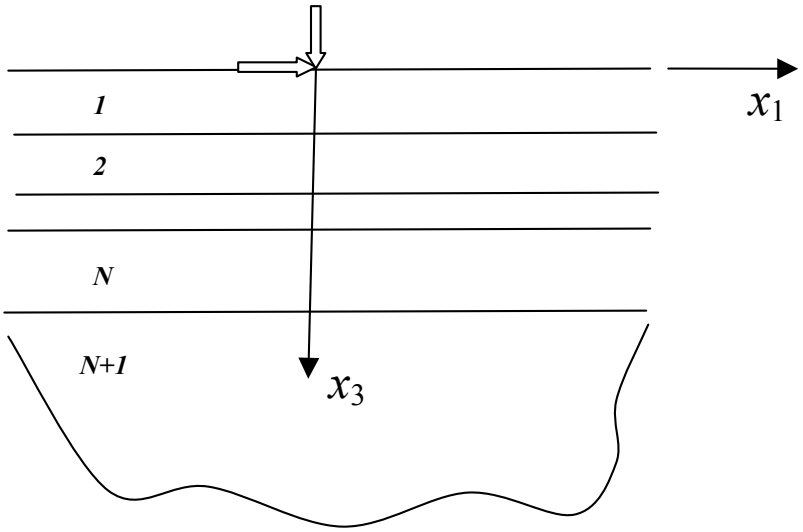

Figure A. Stack of N parallel elastic layers over a 3D half-space.

Vertical force at the surface of a stratified half-space

Consider a unit vertical harmonic point force on the otherwise free surface at $z = 0$. Due to the axial symmetry of problem all results depend on *z* and *r*, the radial horizontal coordinate. For this loading case the normal and the shear stresses should be

$$\sigma_{zz} = -1\delta(x)\delta(y)e^{i\omega t}, \text{ and } \sigma_{zr} = 0, \tag{A1}$$

where $\delta(\bullet)$ = Dirac delta function. Thus we can write

$$\delta(x)\delta(y) = \frac{1}{4\pi^2}\int_{-\infty}^{\infty}\int_{-\infty}^{\infty} e^{ik_x x}e^{ik_y y}dk_x dk_y = \frac{1}{4\pi^2}\int_0^{2\pi}\int_0^{\infty} e^{ikr\cos(\theta-\varphi)}kd\varphi dk = \frac{1}{2\pi}\int_0^{\infty} kJ_0(kr)dk, \tag{A2}$$

where $J_0(\bullet)$ = Bessel function of the first kind and order zero, *r* = radial coordinate and *k* = radial wavenumber. Consider now a single layer, for instance the *j*-th layer. Material properties and space would be the corresponding ones. We will specialize the results for any particular layer. Following Knopoff (1964) and Aki and Richards (1980), the displacements in terms of potentials $\phi(r,z)$ and $\psi(r,z)$, for dilatational and shear waves, respectively, are given by

$$u_r = \frac{\partial\phi}{\partial r} + \frac{\partial^2\psi}{\partial r\partial z}, \text{ and } u_z = \frac{\partial\phi}{\partial z} + \frac{\partial^2\psi}{\partial z^2} + \frac{\omega^2}{\beta^2}\psi \tag{A3}$$

Here u_r and u_z = radial and vertical displacements. Potentials ϕ and ψ are solutions of the reduced wave equations:

$$\nabla^2\phi + \frac{\omega^2}{\alpha^2}\phi = 0, \text{ and } \nabla^2\psi + \frac{\omega^2}{\beta^2}\psi = 0 \tag{A4}$$

respectively. Here α and β = velocities of P and S waves, and ρ = mass density. The potentials that solve Eqs. A4 in layer *j* are

$$\phi = (A_{2j-1}e^{i\gamma(z-z_{j+1})} + A_{2j}e^{-i\gamma(z-z_j)})\,J_0(kr), \text{ and } \psi = (B_{2j-1}e^{i\nu(z-z_{j+1})} + B_{2j}e^{-i\nu(z-z_j)})\,J_0(kr), \tag{A5}$$

respectively. In Eqs. A5 the vertical P and S wavenumbers γ and ν are given by

$$\gamma = \sqrt{\frac{\omega^2}{\alpha^2} - k^2}, \operatorname{Im}\gamma \le 0 \text{ and } \nu = \sqrt{\frac{\omega^2}{\beta^2} - k^2}, \operatorname{Im}\nu \le 0 \tag{A6}$$

respectively. Note that in the potentials ϕ and ψ the odd coefficients (A_{2j-1} and B_{2j-1}) correspond to up-going while the even ones (A_{2j} and B_{2j}) represent down-going waves. The form adopted for the exponentials avoids having growing terms in the representation.
The stresses of interest, σ_{zr} and σ_{zz}, are radial shear and normal stresses for a given *z* as boundary conditions of continuity are to be imposed in horizontal planes. These stresses are obtained from generalized Hooke's law by means of

$$\sigma_{zr} = \mu\left(\frac{\partial u_r}{\partial z} + \frac{\partial u_z}{\partial r}\right), \text{ and } \sigma_{zz} = \lambda\,\Theta + 2\mu\,\frac{\partial u_z}{\partial z}, \tag{A7}$$

respectively. Here $\mu = \rho\,\beta^2$, $\lambda + 2\mu = \rho\,\alpha^2$, and $\Theta = \nabla^2\phi = -(\omega/\alpha)^2\phi \equiv$ dilatation.

For *N* layers over the half-space we have four unknowns for each layer and two for the half space. In that case they correspond to down-going waves. For these 4*N*+2 unknowns an equal number of boundary conditions come from stresses at the uppermost boundary and continuity of normal and radial displacements and stresses at all the interfaces.

For the vertical harmonic, unit point load we have, from Eqs. A1 and A2 that stress components for a given wavenumber *k* at the upper surface $z = z_1 = 0$ must be

$$\sigma_{zz} = \frac{-k}{2\pi} J_0(kr), \text{ and } \sigma_{zr} = 0, \tag{A8}$$

respectively. The boundary conditions for the *N*+1 interfaces come from matching radial and normal displacements and stresses between adjacent layers. The radial functions $J_0(kr)$, and $J_1(kr)$ are common factors in each case so they can be eliminated from the equalities. It will remain to compute the integral over *k*. Details can be found in Sánchez-Sesma *et al.* (2011a).

The horizontal force at the surface of a stratified half-space

The even and odd parts of the field will be modulated by $\cos\theta$ and $\sin\theta$, respectively. In addition of the P and SV waves there are horizontally polarized SH waves. Following Aki and Richards (1980) the respective potentials $\phi(r,z)$, $\psi(r,z)$, and $\chi(r,z)$ are solutions of the reduced wave equations:

$$\nabla^2\phi + \frac{\omega^2}{\alpha^2}\phi = 0\,,\ \nabla^2\psi + \frac{\omega^2}{\beta^2}\psi = 0 \ \text{ and } \nabla^2\chi + \frac{\omega^2}{\beta^2}\chi = 0\,, \tag{A9}$$

respectively. The displacements are given by

$$u_r = \frac{\partial\phi}{\partial r} + \frac{\partial^2\psi}{\partial r\partial z} + \frac{1}{r}\frac{\partial\chi}{\partial\theta},\ u_\theta = \frac{1}{r}\frac{\partial\phi}{\partial\theta} + \frac{1}{r}\frac{\partial^2\psi}{\partial z\partial\theta} - \frac{1}{r}\frac{\partial\chi}{\partial r} \ \text{ and } u_z = \frac{\partial\phi}{\partial z} + \frac{\partial^2\psi}{\partial z^2} + \frac{\omega^2}{\beta^2}\psi \tag{A10}$$

Here u_r, u_θ, and u_z = radial, tangential and vertical displacements. The stresses of interest are $\sigma_{zr}, \sigma_{z\theta}$ and σ_{zz} which correspond to radial and transverse shear and normal stresses on a horizontal plane. They are obtained from generalized Hooke's law by means of

$$\sigma_{zr} = \mu\left(\frac{\partial u_r}{\partial z} + \frac{\partial u_z}{\partial r}\right),\ \sigma_{z\theta} = \mu\left(\frac{\partial u_\theta}{\partial z} + \frac{1}{r}\frac{\partial u_z}{\partial\theta}\right),\ \text{and } \sigma_{zz} = \lambda\Theta + 2\mu\frac{\partial u_z}{\partial z}\,, \tag{A11}$$

respectively. The potentials that solve Eqs. A10 are

$$\phi = \left\{A_{2j-1}e^{i\gamma(z-z_{j+1})} + A_{2j}e^{-i\gamma(z-z_j)}\right\}J_1\cos\theta,\quad \psi = \left\{B_{2j-1}e^{i\nu(z-z_{j+1})} + B_{2j}e^{-i\nu(z-z_j)}\right\}J_1\cos\theta,\ \text{and}$$
$$\chi = \left\{C_{2j-1}e^{i\nu(z-z_{j+1})} + C_{2j}e^{-i\nu(z-z_j)}\right\}J_1\sin\theta. \tag{A12}$$

Expressions for displacements and stresses are too long to be included here but they show a remarkable property; the in the P and SV contributions the *z*-dependent terms for normal and tangential components are identical to the corresponding ones of the vertical load case. Similarly, the two SH shear components (*z*-dependent terms) of the horizontal load case are identical.

At *z*=0 we must enforce that $\sigma_{zz} = 0$, $\sigma_{zr} = -\delta(x)\delta(y)\cos\theta$, and $\sigma_{z\theta} = \delta(x)\delta(y)\sin\theta$. Therefore, considering the identity

$$\delta(x)\delta(y) = \frac{1}{2\pi}\int_0^\infty kJ_0(kr)dk = \frac{1}{2\pi}\int_0^\infty\left\{k\left(J_0 - \frac{J_1}{kr}\right) + k\frac{J_1}{kr}\right\}dk\,, \tag{A13}$$

therefore, we can write for shear stresses

$$\sigma_{zr} = \frac{-1}{2\pi}\left\{k\left(J_0 - \frac{J_1}{kr}\right) + \left(k\frac{J_1}{kr}\right)\right\}\cos\theta = \mu_1\left\{\bullet\,\kappa k\left(J_0 - \frac{J_1}{kr}\right) - \mathrm{i}\nu_1\circ\left(k\frac{J_1}{kr}\right)\right\}\cos\theta\,, \tag{A14}$$

$$\sigma_{z\theta} = \frac{1}{2\pi}\left\{\left(k\frac{J_1}{kr}\right) + k\left(J_0 - \frac{J_1}{kr}\right)\right\}\sin\theta = \mu_1\left\{-\bullet\left(k\frac{J_1}{kr}\right) + \mathrm{i}\nu_1 k\circ\left(J_0 - \frac{J_1}{kr}\right)\right\}\sin\theta\,. \tag{A15}$$

Each boundary condition leads to the pair of equations: $\bullet = -1/2\pi\mu_1$ and $\circ = 1/2\pi\mu_1\mathrm{i}\nu_1$. The first is identical to the corresponding shear stresses equation in the vertical load case. The normal stress contribution leads to the same equations both in vertical and horizontal load. There is also an interesting fact the radial factors have a precise structure that allows construction of the equations. This structure implies that the coefficient matrix is the same for the P and SV contributions of both vertical and horizontal loads.

Finally, the independent term for the tangential load case will give only one non zero term.

Solution of the system

It is then necessary to solve a linear system

$$\mathbf{A}\mathbf{x} = \mathbf{b}\,, \tag{A16}$$

As the matrix for P-SV waves is the same for both the vertical and the horizontal load cases, it is possible to solve simultaneously the two systems of equations. The SH part leads to a smaller system. Details can be found in Sánchez-Sesma *et al.* (2011).

So far in this study the solution is achieved using Gaussian LU factorization and the procedure is stable as no growing exponentials were allowed in the formulation. The choice of the global matrix was dictated by practical considerations. The use of the Kennett's (2001) transmission-reflection recursive approach is contemplated in our current research.

The vector of unknown coefficients includes the coefficients associated to down-going and up-going waves. The structure for the SH contributions is analogous to the P-SV case but with half the dimensions. Once the solution is known one can compute the integrals in the wave number domain.

The imaginary part of Green´s function at the source

The corresponding expressions for both the vertical and the horizontal load cases, evaluated at z=0, r=0 and θ=0 allow to compute the imaginary part of Green function. From the horizontal load case we have

$$\mathrm{Im}[G_{11}(0,0;\omega)] = \mathrm{Im}\left(\int_0^\infty \left\{A_1 e^{-i\gamma_1 h_1} + A_2 + B_1 \nu_1 \mathrm{i} e^{-i\nu_1 h_1} - B_{2_J} \nu_1 \mathrm{i}\right\} \frac{k}{2}\, dk + \int_0^\infty \left\{C_1 e^{-i\nu_1 h_1} + C_2\right\} \frac{k}{2}\, dk\right), \tag{A17}$$

While for the vertical load, we can write

$$\mathrm{Im}[G_{33}(0,0;\omega)] = \mathrm{Im}\left(\int_0^\infty \left\{\gamma_1 A_1 e^{-i\gamma h_1} - \mathrm{i}\gamma_1 A_2 + k^2 B_1 e^{-i\nu h_1} + k^2 B_2\right\} dk\right). \tag{A18}$$

These integrals have to be computed numerically. We studied many cases and found excellent agreement with the calculations using Margerin's (2009) approach. A very fine discretization is required in the integration, particularly at lower frequencies. The various issues of optimization of this approach are subjects of our current research.

APPENDIX B

THE IMAGINARY PART OF GREEN FUNCTION AT THE SURFACE LOAD POINT. THE LAYERED 1D ELASTIC CASE

Consider a 1D layered medium. Assume a set of N horizontal elastic layers overlaying a half-space. Layer j is defined at $z_j \le z \le z_{j+1}$ such that $h_j = z_{j+1} - z_j$ = thickness of layer. For the uppermost layer we have $z_1 = 0$, while z_{N+1} is the top of half-space (see Fig. 2). Now the aim is to compute the imaginary part of Green function for the 1D case. The solutions for the P and S cases are equivalent and are both scalar as there are no mode conversions. Therefore, it suffices to consider the acoustic case.

Consider first a 1D homogeneous elastic medium subjected to a concentrated harmonic loading at depth $z_{\mathbf{A}}$, $\delta(z - z_{\mathbf{A}})\exp(-\mathrm{i}\omega t)$. For simplicity in the case of a 1D space, we use z as the vertical coordinate, instead of x_3 as in the general expression in the case of a 3D space. We can write the governing equation for the Green function or fundamental solution as follows:

$$\frac{\partial^2 G}{\partial z^2} + k^2 G = \frac{-1}{\rho c^2}\delta(z - z_{\mathbf{A}})\,, \tag{B1}$$

where $k = \omega / c$ = wavenumber, $\omega =$ circular frequency, ρ = mass density, and c = wave propagation velocity which can be either α for P waves or β for S waves, and the associated motion is either vertical or horizontal, respectively. Without lack of generality we will refer the Green functions to these cases using $G = G_{11}^{1\mathrm{D}}$ for the horizontal motion and $G = G_{33}^{1\mathrm{D}}$ for the vertical one. In other words, G is representing Green functions in one of the three directions. For the 1D case in unbounded medium we have:

$$G_\infty(z_B, z_A; \omega) = \mathrm{i}(2\rho c^2 k)^{-1} \exp(\mathrm{i}kr), \tag{B2}$$

as it can be verified by direct substitution in Eq. B1. In Eq. B2, $r = |z_A - z_B|$ and z_A and z_B are the receiver and source depths, respectively. The time dependence is given by the factor $\exp(-\mathrm{i}\omega t)$ that has been omitted here and hereafter. Then the imaginary part of 1D Green function is then

$$\mathrm{Im}[G_\infty(z_A, z_B; \omega)] = (2\rho c^2 k)^{-1} \cos kr. \tag{B3}$$

A layer on a half-space

Consider a layer in the region $0 \le z \le h$ such that it overlays a half-space, as shown in Figure B. Consider the source to be at $z = 0$, and assume that a harmonic load is applied there, while the Neumann boundary condition (null derivative with respect to z) is also applied at the free surface, and for the bottom at $z=h$ continuity of field and "stress" is required.

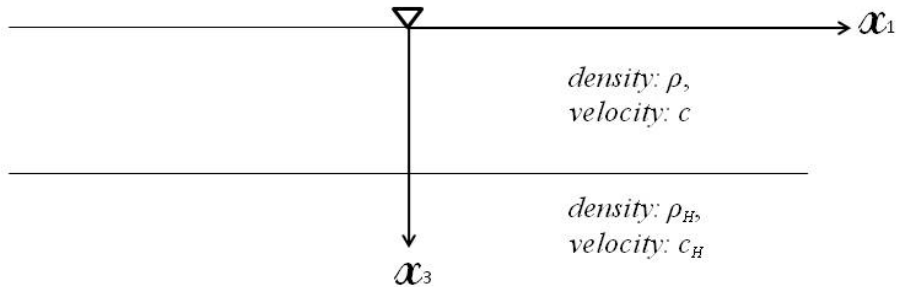

Figure B. Layer of thickness h overlaying a half space.

For this 1D layered problem several theoretical relationships pertaining to GFR from correlations have been pointed out by Nakahara (2006b). He explored several configurations and extended Claerbout's (1968) treatment to receivers that are vertically apart. However, in this study we consider only a surface receiver. The Green function for a surface source is a solution of Eq. B1 subjected to the said boundary conditions. It can be written as:

$$G(z,0;\omega) = \mathrm{i}(\rho c^2 k)^{-1} \exp(\mathrm{i}kz) + A\cos kz, \tag{B4}$$

where the first term accounts for the field from the harmonic unit source at the surface. It is twice the value for an infinite domain. The second term represents the effect of half space and does not induce stress at $z = 0$. By imposing the appropriate conditions that at the bottom and assuming that the radiation toward the half space is of the form $B\exp(\mathrm{i}\omega z/c_H)$, it is possible to show that

$$\mathrm{Im}[G(0,0;\omega)] = (4\rho_H c_H \omega)^{-1} \left\{ \frac{4}{\cos^2 kh + \eta^2 \sin^2 kh} \right\}, \tag{B5}$$

where $\eta=\rho c/\rho_H c_H$ is the impedance ratio of a layer and a half-space. We recognize the quantity within brackets as the square of the absolute value of the surface response to a unit incident harmonic wave from the half space, the so-called transfer function, $TF(\omega)$. We may then write

$$\mathrm{Im}[G(0,0;\omega)] = (4\rho_H c_H \omega)^{-1} |TF(\omega)|^2. \tag{B6}$$

This means that the imaginary part of the response at the free surface due to a source on the same surface can be calculated from the transfer function of the vertically incident body wave from the half space. The above result also holds for a stack of acoustic layers. Details can be found in Kawase *et al.* (2011). For the 1D elastic case it suffices to substitute c with α or β in the case of P or S waves, respectively. Displacements will then be vertical or horizontal corresponding to each case. This result is implicit both in Claerbout's (1968) and Nakahara's (2006b) developments. However, to the best of our knowledge the relationship between the imaginary part of a 1D Green function at the surface of a surface source and the transfer function for an incoming unit wave from a half space has not been pointed out before Kawase *et al.* (2011).